PUBLISHED BY

INTECH

open science | open minds

World's largest Science,
Technology & Medicine
Open Access book publisher



2750+
OPEN ACCESS BOOKS



95,000+
INTERNATIONAL
AUTHORS AND EDITORS



88+ MILLION
DOWNLOADS



BOOKS
DELIVERED TO
151 COUNTRIES

AUTHORS AMONG
TOP 1%
MOST CITED SCIENTIST



12.2%
AUTHORS AND EDITORS
FROM TOP 500 UNIVERSITIES



Selection of our books indexed in the
Book Citation Index in Web of Science™
Core Collection (BKCI)

Chapter from the Book *Environmental and Industrial Corrosion - Practical and Theoretical Aspects*
Downloaded from: http://www.intechopen.com/books/environmental-and-industrial-corrosion-practical-and-theoretical-aspects

Interested in publishing with InTechOpen?
Contact us at book.department@intechopen.com

Chapter 6

A Comparative Study Between Different Corrosion Protection Layers

Adina- Elena Segneanu, Paula Sfirloaga, Ionel Balcu, Nandina Vlatanescu and Ioan Grozescu

Additional information is available at the end of the chapter

http://dx.doi.org/10.5772/52985

1. Introduction

Corrosion is known as the destruction of materials due to interaction with corrosive environment. The destruction caused by metallic corrosion has become a serious problem in the world economy. Metallic corrosion is in most cases an electrochemical process occurring between a metal and its environment involving oxidation and reduction reactions.

There are two general classifications of corrosion which cover most of the specific forms. These are: direct chemical attack and electrochemical attack. In both types of corrosion the metal is converted into a metallic compound such as an oxide, hydroxide or sulphate. The corrosion process always involves two simultaneous changes: the metal that is attacked or oxidized suffers what may be called anodic change, and may be considered as undergoing cathodic change.

Direct Chemical Attack: Direct chemical attack, or pure chemical corrosion, is an attack resulting from a direct exposure of a bare surface to caustic liquid or gaseous agents. Unlike electrochemical attack where the anodic and cathodic changes may be taking place a measurable distance apart, the changes in direct chemical attack are occurring simultaneously at the same point.

The appearance of the corrosion varies with the metal. On aluminum alloys and magnesium it appears as surface pitting and etching, often combined with a gray or white powdery deposit. On copper and copper alloys the corrosion a greenish film, on steel reddish rust. When the gray, while, green, or reddish deposits are removed, each of the surfaces may appear etched and pitted, depending upon the length of exposure and severity of attack. If these surface pits are not too deep, they may not significantly alter the strength of the metal,

INTECH
open science | open minds

© 2012 Segneanu et al.; licensee InTech. This is an open access article distributed under the terms of the Creative Commons Attribution License (http://creativecommons.org/licenses/by/3.0), which permits unrestricted use, distribution, and reproduction in any medium, provided the original work is properly cited.

however, the pits may become sites for crack development. Some types of corrosion can travel beneath surface coatings and can spread until the part fails.

Corrosion of steel or iron substrates can be slowed by coating the metal with different protective coatings. Porphyrins and multifunctional nanocomposites are examples of such coatings. Incorporation of organic or inorganic particles in the protective layers improves the physico-chemical properties [1].

Aluminum is an active metal and is naturally passivized forming an aluminum oxide film (Al_2O_3) on the metal surface. The oxide film can protect aluminum from corrosion in natural and some acid environments; however, it is expected to dissolve in alkalizes.

When oxygen is present (in the air, soil, or water), aluminum instantly reacts to form aluminum oxide. This aluminum oxide layer is chemically bound to the surface, and it seals the core aluminum from any further reaction. This is quite different from oxidation (corrosion) in steel, where rust puffs up and flakes off, constantly exposing new metal to corrosion.

Aluminium oxide is an amphoteric oxide (can react as either an acid or base) of aluminium with the chemical formula Al_2O_3. It is also commonly referred to as alumina, corundum, sapphire, ruby or aloxite in the mining, ceramic and materials science communities. It is produced by the Bayer process from bauxite. Its most significant use is in the production of aluminium metal, although it is also used as abrasive due to its hardness and as a refractory material due to its high melting point [2].

Components	[%]
Al_2O_3	99.2
SiO_2	0.06
Fe_2O_3	0,04
Na_2O	0.40
CaO	0.05

Table 1. Alumina characteristics

Alumina coatings are widely used in a range of industrial applications to improve corrosion protection, wear and erosion resistances, and thermal insulation of metallic surfaces. Refined alumina surfaces with long-term use are obtained from various efficient and adjustable processes. It can be seen that cost efficient arc-sprayed Al coatings post-treated by plasma-electrolytic oxidation (PEO) form Al_2O_3 -layers with remarkable corrosion protection, hardness, bonding strength, and abrasion resistance, as well as with the extended service time. The properties of these coatings are compared with alumina coatings obtained by flame spraying and atmospheric plasma spraying.

The type of corrosion observed on aluminum alloys are as follows:

a. *General Dissolution:* This occurs in strongly acidic or strongly alkaline solutions though there are specific exceptions. Certain inorganic salts (for example, aluminum ferric and zinc chlorides) hydrolyze in solution to give acidic or alkaline reaction and thus cause

general dissolution. Lower alcohols and phenols in anhydrous condition do not allow protective layer to form and cause corrosion. Also at temperatures above 90ºC, the metal is uniformly attacked by aqueous systems.

b. *Pitting:* This is most commonly encountered form of aluminum corrosion. In certain, near neutral aqueous solutions, a pit once initiated will continue to propagate owing to the solution within the pit becoming acidic and the alumina not able to form a protective film close to the metal. Solutions containing the chlorides are very harmful in this respect particularly when they are associated with local galvanic cells, which can be formed for example by deposition of copper from solution or by particles such as iron unintentionally embedded in the metal surface. As little as 0.02 parts per million of copper in hard water could initiate pitting, although more is required for soft water. Aluminum is corroded by sea water. In alkaline media, pitting may occur at mechanical defects in the oxide. The aluminum alloys weather outdoors to grey color which deepens to black in industrial atmospheres.

c. *Intercrystalline Corrosion:*This is also electro thermal in nature, the galvanic cell being formed because of some heterogeneity in the alloy structure which may arise from certain alloying elements present.

d. *Stress Corrosion:*This form of corrosion is of limited occurrence with only aluminum alloys, in particular the higher strength materials such as the Al-Zn-Mg-Cu type and some of the Al-Mg wrought and cast alloys with higher magnesium content. The occurrence of stress corrosion increases in these alloys after specific low temperature heat treatments such as stove enameling.

e. *Bimetallic Corrosion*:Aluminum is anodic to many metals and when it is joined to them with a suitable electrolyte, the potential difference causes a current to flow and considerable corrosion can result. In some cases surface moisture on structures exposed to an aggressive atmosphere can give rise to galvanic corrosion. In practice, copper, brasses and bronzes in marine conditions cause most trouble. The danger from copper and its alloys is enhanced by the slight solubility of copper in many solutions and its subsequent redepositions on the aluminum to set up local active cells.

Contact with steel is comparatively less harmful. Stainless steels may increase attack on aluminum notably in sea water or marine atmospheres but the high electrical resistance of the two surface oxide films minimize bimetallic effects in less aggressive environments. With salts or heavy metals notably copper, silver and gold, the heavy metal deposits on to the aluminum subsequently causes serious bimetallic corrosion [3].

Pitting corrosion is the most commonly encountered form of localized corrosion of aluminum. This type of corrosion is difficult to detect because pits are small and often covered by corrosion products on the metal surface. The mechanism of pitting corrosion is so complicated that it is not completely understood even today. Pitting corrosion for aluminum occurs in media with a pH between 4 and 8. Generally, pitting corrosion consists of the initiation and the propagation stages. Figure 2 shows the mechanism of pitting corrosion of aluminum. In the initiation stage, chloride ions (Cl^-) or other aggressive anions such as bromide and iodide

anions break down the passive film by absorbing on the aluminum surface covered oxide film resulting in formation of micro-cracks. These corrosive anions and corrosion products result in acidic solution within the rupture of the film due to hydrolysis which becomes an active corroding anode.

The pitting potential Epit is the critical potential indicating the relative resistance to pitting corrosion. Pitting occurs above the pitting potential Epit.

The chloride ions can penetrate into the oxide film causing film breakdown and dramatically decrease the pitting potential resulting in lower resistance of pitting corrosion.

After pitting occurs the pits will continue to develop as a self-propagating mechanism. Aluminum at the bottom of the pits will continue to be oxidized because the pits become the anode and produce Al^{3+}. The oxidation reaction at the pit's bottom is given by:

$$2Al \rightarrow 2Al^{3+} + 3e^{-} \quad (1)$$

The positive ions Al^{3+} will react with negative anions such as Cl^{-} resulting in acid chloride solution at the inside of pits. The acid pit solution can be concentrated up to a pH < 3 by further anodic dissolution. The aluminum dissolution process leads to self-propagating of pit growth because the concentrated acid pit solution becomes very corrosive.

Phosphogypsum is a waste product resulted from the process of obtaining the phosphoric acid from apathy and phosphorite by extraction with sulphuric acid.

$$Ca_5F(PO_4)_3 + 5H_2S0_4 + 10H_2O = 3H_3P0_4 + 5CaS0_4 \cdot 2H_20 + HF \quad (2)$$

This waste product is a very fine, wet and friable sand with characteristics dependant both on the origin of the ores as well as the various treatments applied to it. Regarding the crystalline structure, there are 4 types of phosphogyps: acicular crystals (80-500 mm); tubular crystals (40-200 mm); compact crystals; spherical polycrystallinic aggregations (50-100 mm).

Components [%]	Origin:	
CaO	33,31	32,68
SO_3	46,18	44,75
SiO_2	0,23	0,72
P_2O_5	0,84	1,16
H_2O	18,70	18,98

Table 2. The chemical composition of phosphogypsum

Phosphogypsum is used, as an additive, up to 10-15% compared to the binder (ash: lime) in the composition of light masonry blocks. Phosphogypsum can be used with soda as sul-

http://dx.doi.org/10.5772/52985

phate activator, for the mixed alkaline – sulphate activation of ash, in a mixture (ash: lime: phosphogypsum) for stabilizing foundation lands.

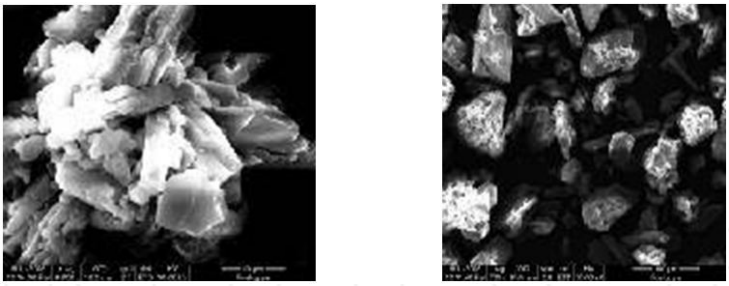


Figure 1. SEM micrographs of phosphogypsum films, 30 μm

Phosphogypsum is often used interchangeably in the research literature with the terms chemical, synthetic, waste or by-product gypsum, which is produced as solid chemical hazardous waste or by-product in industries, by wet or dry processes (sulphuric acidulation of phosphate rocks).

The disposal of phosphogypsum was very simple matter in the early days of industry, as plants had very low capacities (often producing only 25 tons per day of P_2O_5 versus a typical plant today is rated at one kilo tons per day and about up to five kilo tons per day) and environmental concerns and regulations were insignificant. Therefore, phosphogypsum is categorized as hazardous waste in Environmental Protection Agency (EPA) and under category 16 of hazardous waste (Management and Handling) rules 1989 framed by Government of India.

The proper utilization of phosphogypsum is imperious necessary to solve environmental and disposal problems. In different countries attempts have been made from time to time to find ways and means of utilizing phosphogypsum and therefore disposing significant quantity of waste. Concrete, which is a very important constituent of modern construction, is already adopted for waste management system, with exemplary applications like High Volume Fly ash (HVFA) technique. Indeed, concrete in particular is being used as a construction material of a number of waste disposal units, be they for operation, processing or storage of wastes [5,6,7,8].

The goal of this study is to develop of two different nanocomposite materials composed by porphyrin, a granular material (alumina or phosphogypsum) and alkyd paint:

i. porphyrin, a granular material (alumina) and paint (grey varnish paint and yellow alkyd paint);

ii. porphyrin and a granular material (phosphogypsum) and paint (grey varnish paint and yellow alkyd paint).

The anticorrosive properties of these multifunctional systems have been comparatively investigated on carbon-steel electrodes.

The porphyrin type was another parameter that was considered for determining effectiveness of the nanocomposite materials.

In our studies we used two types of modified porphyrins: Na_4TFPAc porphyrin ($C_{44}H_{26}N_4Na_4O_{12}S_4 \times H_2O$) and H_2TPP porphyrin. These porphyrins were dissolved in alkaline, acid and organic solutions (KOH, H_2SO_4 and benzonitrile) as follows:

1. 0.2 g of Na_4TFPAc porphyrin ($C_{44}H_{26}N_4Na_4O_{12}S_4 \times H_2O$) dissolved in 40 ml 10% KOH, mentioned from this point forward as system I;
2. 0.2 g of Na_4TFPAc porphyrin ($C_{44}H_{26}N_4Na_4O_{12}S_4 \times H_2O$) dissolved in 40 ml 10% H_2SO_4, mentioned from this point forward as system II;
3. 0.2 g of H_2TPP porphyrin (5, 10, 15, 20 tetrakis 4 phenyl-21H, 23H) dissolved in benzonitrile, mentioned from this point forward as system III.

The working electrode is the carbon-steel (FeC) electrode with a 0.13 cm^2 active surface; the counter electrode is made of platinum with a 0.31 cm^2 active surface and the reference electrode is the saturated calomel electrode (SCE). All these electrodes are connected to the potentiostat. As base electrolyte we used 20% Na_2SO_4.

The voltammetry measurements were carried out at electrochemical potentials ranging between -1,000 ÷ 2,500 mV and a sweep rate of 100mV/s. The electrode was treated with 5,10,15,20 tetrakis (4 phenyl)-21H, 23H porphyrin (H_2TPP) dissolved in 40 ml benzonitrile. The immersion time was 5 minutes.

Through corrosion tests we determined the resistance of both types of coatings as corrosion inhibitors by cyclic voltammetry and salt spray chamber.

2. Experimental

Electrochemical techniques are powerful tools to provide a better understanding of corrosion phenomena. Mansfeld et al have studied these electrochemical processes and developed a number of electrochemical methods to characterize the corrosion resistance of different metals and alloys [14-16].

Through cyclic voltammetry and Tafel tests we compared the porphyrin systems and determined the best one. Using this system we determined the resistance of alumina and phosphogyps as corrosion inhibitors through the salt spray corrosion test ASTM B 117 [9]. The apparatuses used were: the PGZ 402 Dynamic EIS Voltammetry potentiostat with VoltaMaster 4 software version 7.08 manufactured by Radiometer Copenhagen and the DCTC 600 salt spray chamber manufactured by Angelantoni Industrie (Figure 7).

In order to determine the resistance of alumina and phosphogyps as corrosion inhibitors, we used the DCTC 600 dry salt spray chamber and the ASTM B 117 method. The test lasted 14

http://dx.doi.org/10.5772/52985

days. The 5% NaCl solution was prepared using 1 kg of pure NaCl dissolved in 20 liters of distilled water.

Following the studies, we applied the improved method of dipping the electrode in paint before and after passing through the granular material (alumina or phosphogypsum), thus obtaining the multifunctional system: porphyrin (0.2 g H_2TPP/40 ml benzonitrile) + 2 ml paint + 0.9 ÷ 1.8 g alumina and porphyrin (0.2 g H_2TPP/40 ml benzonitrile) + 2 ml paint + 0.9 ÷ 1.8 g phosphogypsum.

We used two types of paint: grey varnish paint and yellow alkyd paint (named yellow paint).

Alkyd paint	
Aspect	homogeneous liquid, viscous
Density 23°C	0, 94 ± 0,05 g/ml
Flow time	55 -70s
Nonvolatile substances, 0,2- 0,3g, 105°C ;10 min	min. 50 %
Film characteristics :	
Glaze 60°, min.	82 %
Drying time 23 ±2°C, 50±5 % Relative humidity: - Drying time to touch -(TipB) -Drying time in depth - (TipD)	 2 hours 5 hours
Liquids Resistance: water, detergent pH = 7, HCl 3%, ethanol 25%, mineral oil	good, no changes after 24 hours
Elasticity, min.	6mm

Table 3. Characteristics of alchidic paint

3. Results and Discussion

Evaluation of nanocomposite materials by cyclic voltammetry and Tafel tests for an immersion time 5 minutes

From the plots obtained through ciclic voltammetry we determined the peak current (i_{peak}) and peak potential (ε_{peak}) – for increasing and decreasing polarisation, respectively – as well as the passivation potential (ε_{pas}), passivation current (i_{pas}) and oxygen release potential (ε_{O2}). From the Tafel tests we determined the corrosion current (i_{cor}), polarisation resistance (Rp), the corrosion rate (v_{cor}) and the correlation coefficient (C).

The cyclic voltammograms and the Tafel tests are shown in figures 4, 5, 6 and 7.

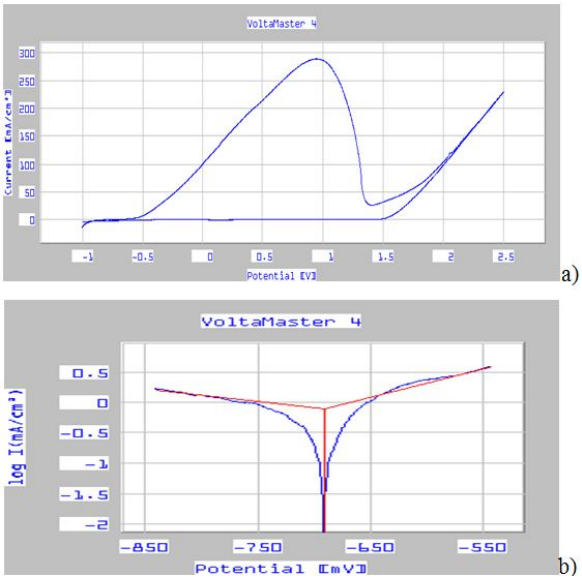


Figure 2. Uncoated carbon-steel electrode; 20% Na_2SO_4 support electrolite; polarisation speed – 100 mV/s; 25°C temperature. a – cyclic voltammogram; b – Tafel test

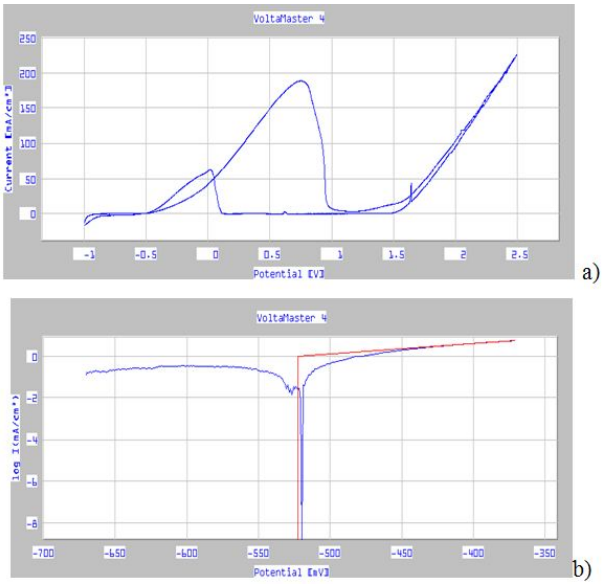


Figure 3. Coated FeC electrode; system I; a - cyclic voltammogram; b -Tafel test

http://dx.doi.org/10.5772/52985

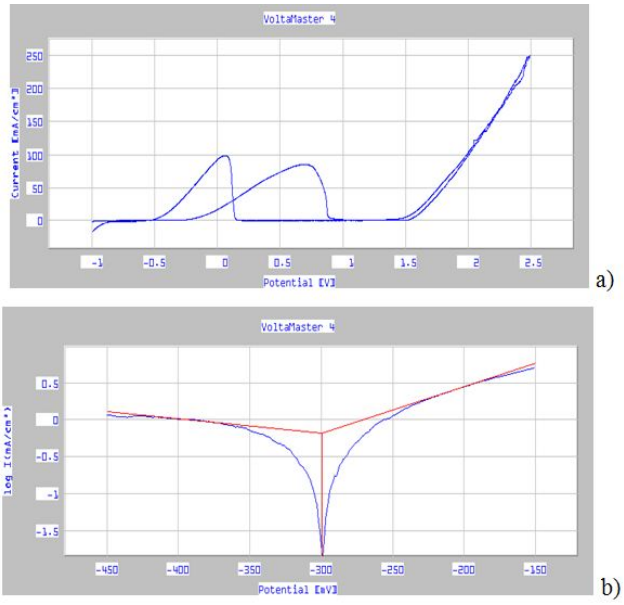


Figure 4. Coated FeC electrode; system II; a – cyclic voltammogram; b –Tafel test

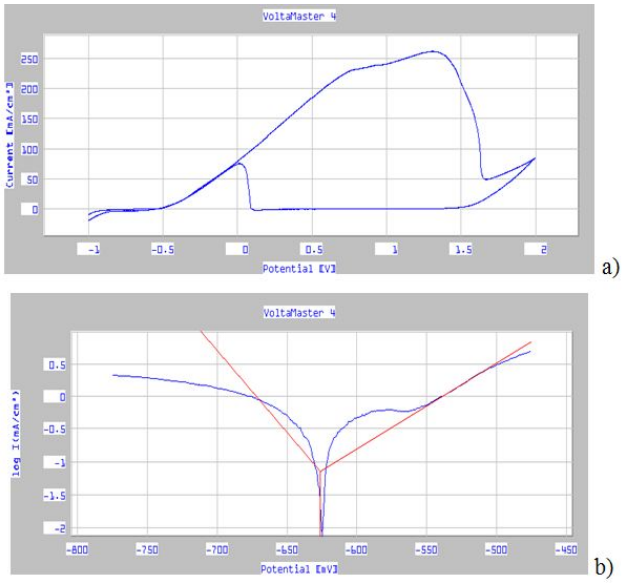


Figure 5. Coated FeC electrode according to system III; a – cyclic voltammogram; b –Tafel test

Table 4 shows the values of different parameters for uncoated and coated electrodes resulted from the cyclic voltammograms shown in figures 4a, 5a, 6a, 7a and table 3 shows the values of different parameters for uncoated and coated electrodes resulted from the Tafel tests shown in figures 4b, 5b, 6b, 7b.

Parameters	Electrodes			
	Uncoated	System I	System II	System III
$i^{\rightarrow}_{peak}$ [mA/cm^2]	290	280	90	80
$\varepsilon^{\rightarrow}_{pic}$ [mV]	900	750	600	1300
$i^{\leftarrow}_{peak}$ [mA/cm^2]	-	60	100	85
$\varepsilon^{\leftarrow}_{peak}$ [mV]	-	50	100	50
ε_{O2} [mV]	1500	1500	1500	1500
ε_{pas}[mV]	1350	900	850	1600
i_{pas} [mA/cm^2]	25	8	0	50

Table 4. Values of different parameters for uncoated and coated electrodes resulted from the cyclic voltammograms shown in figures 4a,5a, 6a, 7a

The notations used in table 4 are as follows: $i^{\rightarrow}_{peak}$ - peak current density for increasing polarization; $\varepsilon^{\rightarrow}_{peak}$ - peak potential for increasing polarization; $i^{\leftarrow}_{peak}$ - peak current density for decreasing polarization; $\varepsilon^{\leftarrow}_{peak}$ - peak potential for decreasing polarization; ε_{O2} - oxygen release potential; ε_{pas} - passivation potential; i_{pas} - passivation current.

Variation of $i^{\leftarrow}_{peak}$ is correlated with the porphyrin systems. Na_4TFPAc both in NaOH as well as in H_2SO_4 and H_2TPP solutions exhibits a decrease in $i^{\leftarrow}_{peak}$ value.

The peak potential ($\varepsilon^{\leftarrow}_{peak}$) shows a similar evolution: decreased values for system I and II and increase values for system III. There is no variation in the oxygen release potential (ε_{O2}). Passivation potential (ε_{pas}) and passivation current depend on the coating systems. The values decreased for system I and II and increased for system III (20% increase).

Parameters	Electrodes			
	Uncoated	System I	System II	System III
i_{cor} [mA/cm2]	0.9792	0.7666	0.6506	0.0718
v_{cor} [mm/year]	11.48	8.99	7.63	0.842
Rp	50.91	129.51	59.57	47.67
C	0.9962	0.9996	0.9997	1.000

Table 5. Values of different parameters for uncoated and coated electrodes resulted from the Tafel tests shown in figures 4b,5b, 6b, 7b.

http://dx.doi.org/10.5772/52985

The notations used in table 5 are as follows: i_{cor} - corrosion current; v_{cor} - corrosion rate; Rp - polarisation resistance; C - correlation coefficient.

Making a comparison between the treated and untreated electrodes observed a significant decrease in corrosion rate for the treated electrodes resulting in the formation of a passive layer of corrosion protection, also resulting in better adhesion for application of corrosion inhibitor on the surface electrode.

These results indicate that corrosion rate depends on the type of porphyrin system. For system I, there is a corrosion rate increase of about 25%; a corrosion rate decrease of 15 % for system II and a significant corrosion rate decrease of about 10 times for system III, indicating that the surfaces of FeC electrode coated with H_2TPP form an efficient passive corrosion protection layer. The reference corrosion speed is the v_{cor} of the uncoated FeC electrode (8.99 mm/year).

Electrochemistry as a tool for the study of the physical properties of porphyrins has been extensively used recently. The effect of substituents on the oxidation and reduction reactions of the π system of tetraphenylporphyrin (TPP) was investigated by Kadish et al. by cyclic voltammetry in methylene chloride and in other solvent. In all solvents it was found that electron-donating substituents shift the oxidation and the reduction potentials to more positive values. Electron attracting substituents on the other hand, shift the potentials to more negative values. When the $E_{1/2}$ values were plotted vs. the Hammett substituent constant σ a linear free-energy relationship were obtained. Both ring reduction to yield the π anion radical and ring oxidation to yield the π cation radical showed sensitivity to para substitution, and an average value of 0.07 ± 0.01 V was found for the Hammett reaction constant ϱ. The Hammett constants for the oxidation reactions to yield π cation radicals were found relatively more sensitive to para substitution and varied from 0.064 V for free-base TPP (in CH_2C1_2).

The electrode processes (oxidation and reduction) did not satisfy all the diagnostic criteria for reversible charge transfer: [9]

$$(p-X,p-Y)H_2TPP - e^- \leftrightarrow \left[(p-X,p-Y)\ H_2TPP\right]^+ \quad (3)$$

$$(p-X,p-Y)H_2TPP - e^- \leftrightarrow \left[(p-X,p-Y)\ H_2TPP\right]^+ \quad (4)$$

$$(p-X,p-Y)\ H_2TPP + e^- \leftrightarrow \left[(p-X,p-Y)\ H_2TPP\right]^- \quad (5)$$

$$\left[\ (p-X,p-Y)\ H_2TPP\right]^- + e^- \leftrightarrow \left[p-X,p-Y)\ H_2TPP\right]^{2-} \quad (6)$$

Porphyrins are a class of natural pigments containing a fundamental skeleton of four pyrrole nuclei united through the α-positions by four methine groups to form a macrocyclic

structure. Porphyrin is designated also with the nomenclature of porphine. The common meso-substituted porphyrins are tetraphenyl porphyrin (R = phenyl) and ortho, meta or para substituted phenyl porphyrins. Usually, for the mesotetraphenylporphyrin synthesis is used pyrole and an aldehyde such as benzaldehyde, salicylaldehyde, and so on [12].

The porphyrin nucleus is a tetradentate ligand. When coordination occurs, two protons are removed from the pyrrole nitrogen atoms, leaving two negative charges. The porphyrin ring system exhibits aromatic character, containing 22 π-electrons, but only 18 of them are delocalized according to the Hückel's rule of aromaticity (4n+2 delocalized π-electrons, where n=4).

Simple porphyrins with identical substituents in *meso* or β-positions are usually prepared by methods based on monopyrrole condensation (the Rothemund Method), when four identical pyrrole molecules are condensed into a porphyrin in one step.

4. Redox Properties of Tetraphenylporphyrin (H_2TPP)

The use of electrochemical methods to estimate the redox properties of porphyrins is vital for understanding the photochemistry of porphyrins. In general, free-base porphyrins possess two oxidation peaks and two reduction peaks in cyclic voltammetry.

These correspond to the one and two electron oxidation and reduction of the porphyrin π system. The redox properties exhibit a good correlation with the electronegativity or inductive parameter of the central metal atom. Substituents on the porphyrin ring show a good correlation between the redox potentials and the Hamett σ values. The electrochemical band gap corresponds well with the optical band gap determined by the lowest energy absorption in the Q band, indicating that the central metal and substituents equally affect the HOMO and LUMO levels. The number of substituents is also correlated with the shifts in the redox peak positions. Distortion from planarity seems to cause a dramatic change in the oxidation potential. The addition of a redox active metal complicates the overall electrochemical properties of porphyrins, due to the intervening oxidation and reduction potentials of the metal. The change in axial ligand also seems to play an important role in the redox potentials of porphyrins.

Electrochemistry provides valuable insight into the electronic properties of molecules. This technique provides information on the position of the energy levels, in particular the highest occupied molecular orbital (HOMO) and the lowest unoccupied molecular orbital (LUMO) are easily discernable from these measurements. The position of the HOMO of a molecule is probed by determining its anodic potential, while the position of the LUMO is determined by its cathodic potential. These positions can be referenced with respect to the vacuum level by adding 4.7 eV to the onset of the peak (oxidation/reduction) with respect to the ferrocene / ferrocenium (Fc / Fc+) redox couple. The redox properties of porphyrin were performed studies on different types of electrodes [13].

The electrochemical properties of tetraphenylporphyrin are well known. The first oxidation with respect to Fc/Fc+ was determined to be 0.54 V and was determined to be reversible. The

http://dx.doi.org/10.5772/52985

first reduction peak was determined to be located at -1.75 V and was also reversible. These observations correspond well with previously published results. The electrochemical "band-gap" (HOMO – LUMO gap), which was determined by the difference of the $E_{1/2}$ of the anodic and cathodic waves, was determined to be ~ 2.2 eV which corresponds well with the optical gap measured by absorption. Substitution on the *meso*-phenyl groups of TPP has little effect on the charge transport properties of these complexes. Therefore these novel complexes still facilitate whole transport and hinder electron transport. In order to correct this problem, the electron transporting ability must be increased. This can be accomplished by either lowering the LUMO by substitution of electron withdrawing moieties on the pyrroles of the porphyrin or by creating a "molecular wire" in which electrons can flow freely, reducing the barrier for electron injection [10].

In experiments, the efficiency of nanocomposites materials developed as inhibitors for corrosion was tested in salt spray chamber. The corrosion of metallic surface occurs in the aggressive chloride ions attack in the oxide film and the corrosion are propagated according to the following anodic reactions:

$$Al \rightarrow Al^{+3} + 3e \tag{7}$$

$$Al^{+3} + 3H_2O\ Al(OH)_3 + 3H^+ \tag{8}$$

Hydrogen evolution and oxygen reduction are the important reduction processes at the intermetallic cathodes as:

$$2H^+ + 2e \rightarrow H2 \tag{9}$$

$$O_2 + 2H_2O + 4e \rightarrow 4OH \tag{10}$$

According to reaction 2, the pH will decrease as corrosion propagates. To balance the positive charge produced by reactions 1 and 2, chloride ions will migrate into the pit. The resulting HCl formation inside the pit causes in the protective film accelerated the corrosion propagation. It is postulated that, at the critical pitting potential, breakdown occurs by a process of field assisted Cl adsorption on the hydrated oxide surface and formation of a soluble basic chloride salt which readily goes into solution.

5. Evaluation of coatings by exposure to the salt spray test

The table below shows the conditions for testing the anticorrosive coating in salt spray chamber [11].

Type of saline used	NaCl and distilatted water
pH	6,5-7,5
Concentration of the solution	5 %
Spray pressure	60-150 kPa
The amount of saline spray	1-2 ml/h per 80 cm^2
Temperature	25- 40°C
Sample pozition	15° vertical
Time	336 hours

Table 6. Conditions inside the salt spray chamber for testing the anticorrosive coating

In Table 7 are presented the corrosion evolution based on the composition of the protecting film.

PROTECTION FILM COMPOSITION	CORROSION EVOLUTION (h)
H_2TPP + yellow paint + 1,8g Al_2O_3	After 23h: pitting corrosion
H_2TPP + yellow paint + 0,9g Al_2O_3	After 23h: pitting corrosion
H_2TPP+grey varnish paint + 0,9g Al_2O_3	After 48h: uniform corrosion
H_2TPP + grey varnish paint + 1,8g Al_2O_3	After 23h: pitting corrosion
grey varnish paint + 0,9g Al_2O_3	After 25h: pitting corrosion
grey varnish paint + 1,8g Al_2O_3	After 48h: uniform corrosion
yellow paint + 0,9g Al_2O_3	After 23h: pitting corrosion
grey varnish paint + 1,8 g Al_2O_3	After 77h: uniform corrosion
untreated	After 1h: uniform corrosion
H_2TPP + yellow paint + 1,8g phosphogyps	After 23h: pitting corrosion
H_2TPP + yellow paint + 0,9g phosphogyps	After 48h; pitting corrosion
H_2TPP + grey varnish paint + 1,8g phosphogyps	After 144h: uniform corrosion
H_2TPP + grey varnish paint + 0,9g phosphogyps	After 5h; corossion was present in two places in the form of blisters
grey varnish paint + 0,9g phosphogyps	After 48h; uniform corrosion
grey varnish paint + 1,8g phosphogyps	After 77h; uniform corrosion
grey varnish paint + 0,9g phosphogyps	After 23h; uniform corrosion
grey varnish paint + 1,8 g phosphogyps	After 23h; uniform corrosion

Table 7. Corrosion evolution based on the composition of the protecting film

http://dx.doi.org/10.5772/52985

6. Conclusions

- Corrosion speed is mostly decreased in case of the electrode treated with porphyrin, gray varnish paint and 1.8 g phosphogyps.

- The method used for covering the electrodes is also important because when the electrode is diped in paint its surface becomes uniformly covered thus avoiding exogen corrosion.

- The multifunctional system containing phosphogypsum was a better corrosion inhibitor than the one containing alumina.

Author details

Adina- Elena Segneanu*, Paula Sfirloaga, Ionel Balcu, Nandina Vlatanescu and Ioan Grozescu

*Address all correspondence to: s_adinaelena@yahoo.com

National Institute of Research and Development for Electrochemistry and Condensed Matter, INCEMC-Timisoara, Romania

References

[1] Saji, V. S., & Thomas, J. (2007). Nanomaterials for corrosion control. *Current Science*, 92(1), 1.

[2] Harris, C., & Mc Lachlan, R. (1998). Clark, Colin- Micro reform- impacts on films: aluminium case study. Melbourne: Industry Commission

[3] Mahindru, D. V. (2011). Ms Priyanka Mahendru, Protective Treatment of Aluminum and its Alloys. Global Journal of Research in Engineering Version 1.0,, 11(3)

[4] Huang, Y. (2009). Electrochemical Evaluation Of Advanced Anodized Aluminum and Chromate-Free Conversion Coatings. *A Dissertation Presented to the Faculty Of The Graduate School University Of Southern California*.

[5] Environmental Protection Agency. (1999). CFR Part 61: National emission standard for hazardous air pollutants. *National Emission standards for Radon emissions from phosphogypsum stacks, Federal register*, 64(2), 5574-5580.

[6] Jamwal, N. (2000). Blind to danger: Special report. *Down to Earth*, 8(17).

[7] Thakare, R. B., Bhatia, O. P., & Hiraskar, K. G. (2001). Phosphogypsum utilisation in India: Literature survey. *The Indian Concrete Journal*, http://www.icjonline.com, 75(6), 408-410.

[8] Singh, M. (1980). Physio- chemical studies on phosphogypsum for use in building materials. *PhD Thesis, University of Roorkee, Roorkee, India*.

[9] Ulman, A., Manassen, J., Frolow, F., & Rabinovich, D. (1981). Synthesis and Properties of Tetraphenylporphyrin Molecules Containing Heteroatoms Other Than Nitrogen. *Electrochemical Studies Inorg. Chem.*, 20.

[10] Senge, M. O. (2000). *In "The Porphyrin Handbook"; Kadish, K. M., Smith, K. M., Guilard, R., Eds., Academic: New York*, 1, 239-347.

[11] Standard practice for operating salt spray (fog) apparatus. B117-02.

[12] Sharma, R. K., Ahuja, G., & Sidhwani, I. T. (2009). A new one pot and solvent-free synthesis of nickel porphyrin complex. Green Chemistry Letters and Reviews June, , 2(2), 101-105.

[13] Kadish, K. M., & Caemelbecke, E. V. (2003). *J. Solid. State Electrochem*, 7, 254.

[14] Mansfeld, F. (1976). The Polarization Resistance Technique for Measuring Corrosion Currents. In: Fontana MG, Staehle RW, editors. Advances in Corrosion Science and Technology New York: Plenum Press , 6, 163.

[15] Mansfeld, F., & Kendig, M. W. (1984). *Corrosion*, 41, 490.

[16] Mansfeld, F., Han, L. T., Lee, C. C., & Zhang, G. (1998). Evaluation of corrosion protection by polymer coatings using electrochemical impedance spectroscopy and noise analysis. *Electrochimica Acta*, 43, 2933.

INTECH